Peri-graft bone mass and connectivity as predictors for the strength of tendon-to-bone attachment after anterior cruciate ligament reconstruction

Chun-Yi Wen [a,b], Ling Qin [a,b], Kwong-Man Lee [c], Kai-Ming Chan [a,b,*]

[a] Department of Orthopaedics and Traumatology, Faculty of Medicine, The Chinese University of Hong Kong, Hong Kong SAR, China
[b] The Hong Kong Jockey Club Sports Medicine and Health Sciences Centre, Faculty of Medicine, The Chinese University of Hong Kong, Hong Kong SAR, China
[c] Lee Hysan Clinical Research Laboratories, The Chinese University of Hong Kong, Hong Kong

ARTICLE INFO

ABSTRACT

The present study was designed to compare peri-graft bone mass and microarchitecture with tendon-to-bone (T–B) attachment strength after anterior cruciate ligament (ACL) reconstruction in a rabbit model. Surgical reconstruction using digital extensor tendon in bone tunnel was performed on 58 rabbits. Forty-two of the 58 rabbits were sacrificed at week 0, 2, 6 and 12 after operation respectively. The femur–graft–tibia complexes were harvested for pQCT and micro-CT examination to characterize the spatiotemporal changes of peri-graft bone in T–B healing in conjunction with histological examination. The remaining 16 rabbits were euthanized at week 6 and 12 postoperatively (i.e. 8 rabbits for each time point) for pull-out test after micro-CT examination to investigate the relationship between the T–B attachment strength and peri-graft bone mass/microarchitecture. Peri-graft BMD, BV/TV and connectivity was significantly lower at week 6 than those at time zero although there were no significant changes detected in the first 2 postoperative weeks. In addition, peri-graft bone mass and connectivity was significantly lower on the tibial side than those on the femoral side; and osteoclasts accumulated on the surface of peri-graft bone. Grafted tendon was prone to be pulled out from the tibial tunnel with bone attachment; the weakest point of the complexes shifted from the healing interface at time zero to peri-graft bone at week 6 after operation. With reverse of peri-graft bone at week 12 postoperatively, the weakest point shifted to the intra-osseous tendinous portion. The stiffness of T–B attachment correlated with peri-graft BV/TV ($r^2 = 0.68$, $p = 0.001$) and connectivity ($r^2 = 0.47$, $p = 0.013$) at week 6 after operation. T–B healing was a highly dynamic process of emergence and maintenance of peri-graft bone. T–B attachment strength was in relation to peri-graft bone mass and connectivity after ACL reconstruction. The measurement of peri-graft bone should be useful to monitor the quality of T–B healing and guide the postoperative rehabilitation.

© 2008 Elsevier Inc. All rights reserved.

Introduction

Anterior cruciate ligament (ACL) rupture is one of the most common knee injuries in sports medicine. Surgical reconstruction using tendon graft in bone tunnel is frequently performed to restore knee integrity and stability [1]. Tendon–bone (T–B) healing and its attachment strength is the deterministic factor for the outcome of ACL reconstruction [2]. Prediction of T–B healing and its attachment strength is an issue of major clinical importance for the guidance of postoperative rehabilitation and return to activity.
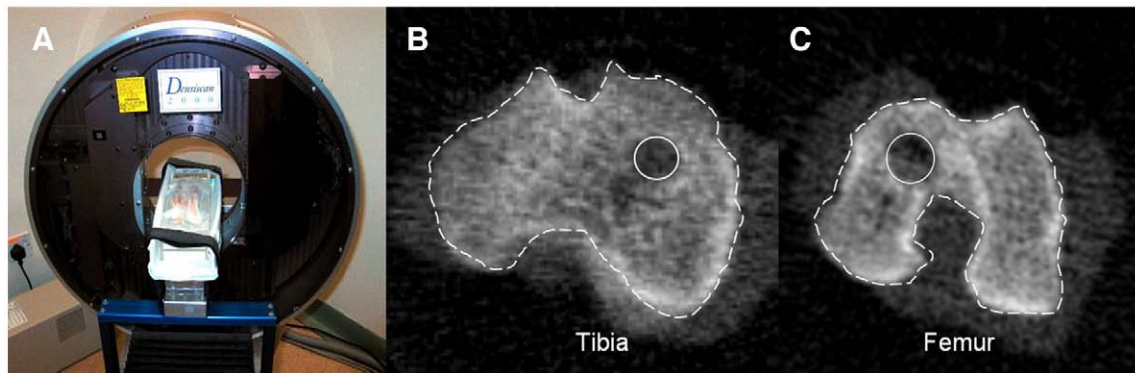
Grassman et al. found that T–B healing in trabeculae-rich femoral tunnel was better than in the marrow-rich tibial tunnel [3]. Recently, it was reported that a decrease of T–B attachment strength was accompanied by bone mineral loss within 6 weeks postoperatively

in a phalangeal bone tunnel of canine [4,5]. Those findings indicated the potential relationships between the quality and quantity of peri-graft bone and T–B healing.

Bone mineral and microarchitecture at a native tendon/ligament-to-bone attachment site play a role in load transfer from tendon/ligament-to-bone [6–10]. It was revealed that bone mineral gradient across ligament-to-bone (L–B) attachment corresponded to regional mechanical properties [6]. Loss of bone mineral at L–B attachment site resulted in impairment of L–B mechanical properties [9,10]. Recently, it was observed that the force of Achilles tendon was transmitted through anisotropic trabeculae to plantar fascia [7]. Changes of microarchitecture of trabeculae indicated the initiation of disorders at T–B attachment site [8]. Naturally, there are no sites in human, where a tendon or ligament goes into a bone tunnel; therefore, there is no native situation analogous to the attachment site of grafted tendon-to-tunneled bone [11]. It remains unknown whether the strength of T–B attachment inside a tunnel was related to bone mineral and microarchitecture in the vicinity of a grafted tendon after ACL reconstruction.

* Corresponding author. Department of Orthopaedics and Traumatology, The Chinese University of Hong Kong, Shatin N.T., Hong Kong SAR, China. Fax: +852 2646 3020.
E-mail addresses: wenchunyi@ort.cuhk.edu.hk (C.-Y. Wen), kaimingchan@cuhk.edu.hk (K.-M. Chan).

Fig. 1. pQCT scan and examination. (A) Distal femur and proximal tibia were scanned perpendicular to the long axis of limb; (B and C) One representative slice in the middle portion of bone tunnel was selected from the tibial (B) and from the femoral side (C) for analysis. On each slice, bone mineral density (within the dotted line) and bone tunnel area (within circle) were measured.

The present study was designed to investigate spatiotemporal changes of BMD and bone microarchitecture in the vicinity of a grafted tendon postoperatively using both pQCT and micro-CT, and compare radiological findings with the pull-out strength of the tendon graft in an ACL reconstruction rabbit model. We hypothesized that the pull-out strength of T–B attachment inside a tunnel related to peri-graft bone mass and microarchitecture after ACL reconstruction. Accordingly, the findings of the present study would provide useful non-invasive imaging modalities for monitoring healing process and quality of T–B healing inside the tunnel after common ACL surgical reconstruction in sports medicine.

Materials and methods

Study design

This experiment was approved by the Research Ethics Committee of the authors' institute (Ref No. CUHK06/004/ERG). Fifty-eight skeletally-mature female New Zealand white rabbit (26-week-old; weight: 3.5–4.0 kg) were used in the present study. Bilateral ACL reconstruction was performed. One reconstructed knee was randomly selected for the subsequent examination in the present study. The contralateral knee was treated by local application of calcium phosphate cement for enhancement of peri-graft bone healing and T–B attachment strength, and the related findings were reported separately [12].
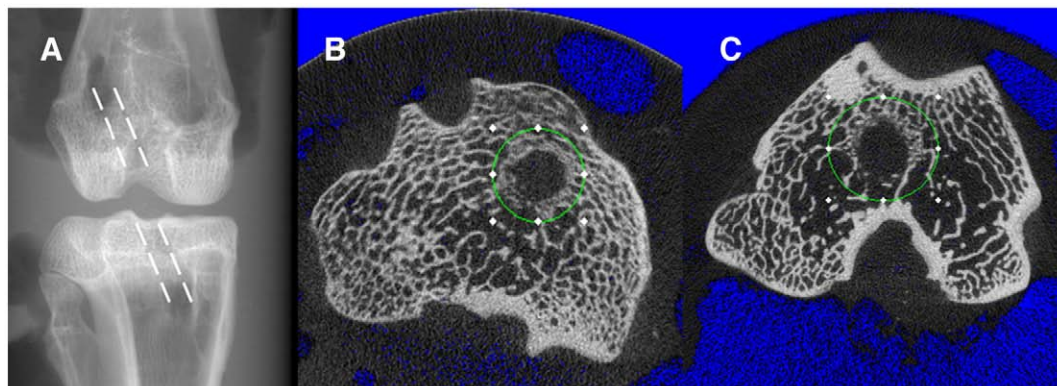
42 of 58 rabbits were sacrificed at week 0, 2, 6 and 12 after operation respectively for pQCT and micro-CT examination to characterize the spatiotemporal changes of peri-graft bone in T–B healing in conjunction with histological examination. 6 rabbits were

sacrificed at time zero (week 0 after operation) for pQCT and micro-CT evaluation and served as the baseline for comparison. The other 36 rabbits were sacrificed at 2, 6 and 12 weeks respectively after surgery (i.e. 12 rabbits for each time point). At each time point, 6 samples were subjected to pQCT evaluation and decalcified histological examination; the other 6 samples were used for micro-CT evaluation and followed by undecalcified histological examination.
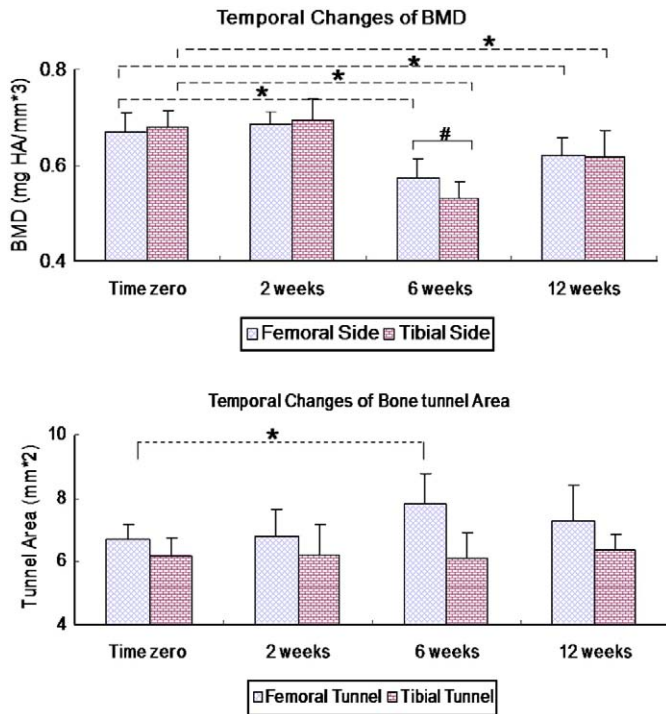
The rest of 16 rabbits were euthanized at week 6 and 12 respectively (i.e. 8 rabbits for each time point). The samples were processed for biomechanical test after micro-CT evaluation to investigate the relationship between the strength of T–B attachment and peri-graft bone mass and microarchitecture. The failure mode was judged by both gross and microscopic examination after the test.

Animal surgery

ACL reconstruction rabbit model was established according to an established protocol by Wang et al. [13]. In brief, the rabbits were operated under general anesthesia with 10% ketamine/2% xylazine (Kethalar, 1mL:1mL) and maintained sedation with 2.5% sodium phenobarbital injected intravenously (Sigma Chemical Co., St. Louis, Mo, USA). The medial parapatella arthrotomy was performed to expose the knee joint. Patella was then dislocated and infrapatella fat pad was removed to expose the joint cavity. ACL was excised and transverse meniscal ligament was also removed. The long digital extensor tendon graft was harvested and graft preparation was done by removing the attached muscle and passing the holding sutures through each end of the tendon graft in an interdigitating whipstitch fashion. Femoral and tibial tunnels were created through the footprint

Fig. 2. Micro-CT scan and analysis. (A) The femoral and tibial tunnel, showed by white dotted line, were scanned perpendicular to the long axis of limb; (B and C) The region of interest of 6mm diameter was defined to cover bone tunnel on both the tibial (B) and femoral side (C).

Fig. 3. Temporal changes of BMD and tunnel area on the femoral and tibial sides. BMD decreased at 6 weeks and partially reversed at 12 weeks postoperatively on both femur and tibia in comparison with that at time zero (* represent significant changes with healing over time at the level of $p < 0.05$ for *post hoc* test after two-way ANOVA analysis). BMD on the femoral side was higher than that on the tibial side at 6 weeks after surgery ($^{\#}p < 0.05$); however, the area of the femoral tunnel showed transient enlargement at 6 weeks postoperatively (*$p < 0.05$); no significant changes of the tibial tunnel area were detected.

of original ACL. The graft was then inserted and routed through the bone tunnels via the holding sutures. The graft at the extra-articular exits of the tunnel was fixed with maximum tension to the neighboring soft tissue by secure knots. The wound was closed in layers and wrapped with dressing. The rabbits were allowed for free cage movement after surgery. The femur–graft–tibia complexes were harvested for the subsequent examinations.

pQCT evaluation

The volumetric BMD (mg/m^3) in the vicinity of the grafted tendon on both distal femur and proximal tibia were measured using a multi-layer pQCT (Densiscan 2000, Scanco Medical, Brüttisellen, Switzerland) based on an established protocol [4,14]. In brief, the samples assumed a supine position, with the leg fully extended in an anterior–posterior position. The samples were secured in a suitable radiolucent cast to fix knee joint in the position of full extension for scanning Fig. 1A. An anterior–posterior scout image was obtained under the

peel mode and a joint line was set as the reference; the cross-sectional slices were then taken perpendicular to the long axis of the limb with slice thickness of 1mm and voxel size of 0.3mm/pixel. As showed in Figs. 1B and C, the slice in the middle portion of bone tunnel was selected on distal femur and proximal tibia respectively; in one of the selected slice, BMD and tunnel area was measured. A standard IBT phantom measurement was performed daily with three measurement values within the given reference ranges provided by the manufacturer. The repeated measurements of BMD were conducted in a pilot study that showed a precision error of 1.2%.

Micro-CT evaluation

The peri-graft bone volume and architecture was evaluated using a high-resolution micro-CT (μCT-40, Scanco Medical, Brüttisellen, Switzerland) according to our established protocol [15,16]. In brief, the samples were placed with their long axes in the vertical position and immobilized with a foam pad in a cylindrical sample holder. The continuous scans were prescribed perpendicular to the long axis of the limb at an isotropic resolution of 30 μm^3. A region of interest (ROI) of 6mm in diameter was user-defined to cover bone tunnel and the entire tunnel was used for subsequent analysis (Fig. 2). The same ROI was used in all of the samples of week 2, 6 and 12, postoperatively. The acquired 3D data set was convoluted with a 3D Gaussian filter with a width and support equal to 1.2 and 2, respectively. Bone was segmented from the marrow and soft tissue for subsequent analyses using a global thresholding procedure. A threshold equal to or above 210 represented bone tissue; a threshold below 210 represented bone marrow and soft tissue. The parameters of bone mass and microarchitecture were evaluated using the built-in software of micro-CT, including the fraction of bone volume/tissue volume (BV/TV), connectivity density (Con.D), degree of anisotropy (D.A), structure model index (SMI), trabecular number (Tb.N), trabecular thickness (Tb.Th), and trabecular spacing (Tb.Sp).

Decalcified histological examination

After pQCT evaluation, the specimens were fixed in 10% neutralized formalin, and decalcified with 9% formic acid for 3 weeks. Longitudinal sections of 7 μm thick were cut along the long axis of the bone tunnel. The sections were stained with Hematoxylin–Eosin (H and E); the osteoclasts distribution in peri-graft bone healing and T–B collagen fiber reconnection was examined under a microscopic imaging system (Leica Q500MC, Leica Cambridge Ltd., Cambridge, UK).
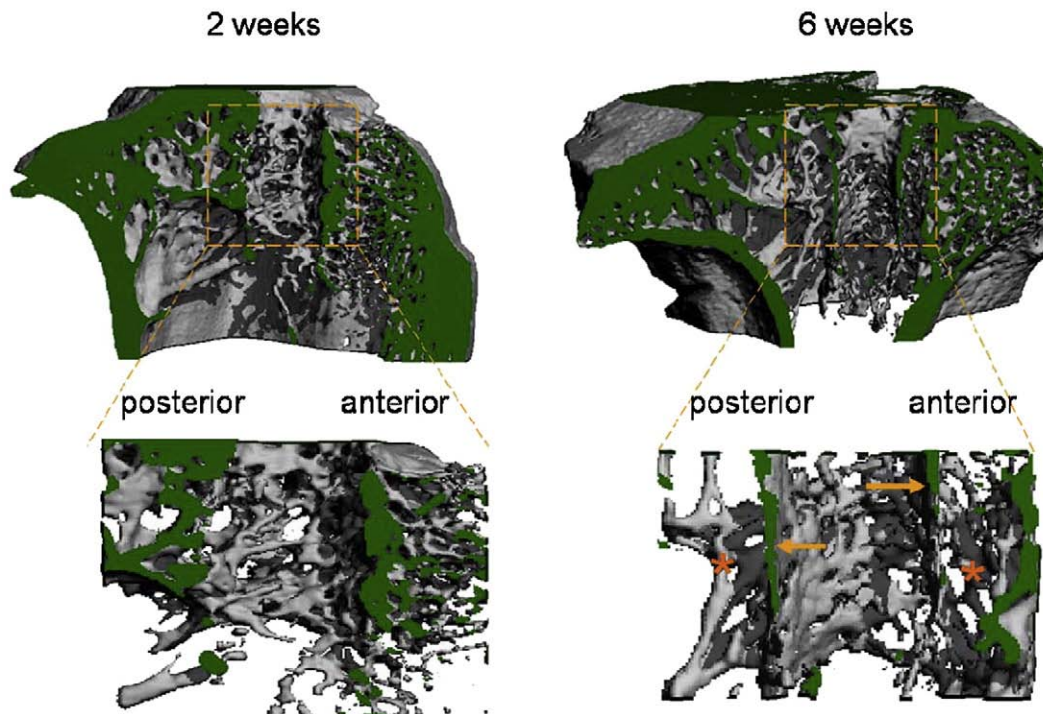
Undecalcified histological examination

Peri-graft bone mineral apposition rate was investigated via sequential fluorescent dyes labeling *in vivo* using an established protocol [17]. In brief, three different fluorescent dyes: xylenol orange (90 mg/kg body weight), calcein green (10 mg/kg body weight, both from Sigma-

Table 1
Spatiotemporal changes of peri-tendon bone mass and microarchitecture.

Time point/sites	Time zero		2 weeks		6 weeks		12 weeks	
	Femoral side	Tibial side	Femoral side	Tibial side	Femoral side	Tibial side	Femoral side	Tibial side
Bone volume/tissue volume (0–1)*	0.18 ± 0.02	0.20 ± 0.02	0.17 ± 0.02	0.18 ± 0.03	$0.15 \pm 0.04^{\#}\downarrow$	$0.12 \pm 0.03^{\#}\downarrow$	0.20 ± 0.03	0.21 ± 0.03
Connectivity density* (1/mm^3)	4.52 ± 0.75	4.62 ± 0.48	4.45 ± 0.56	4.58 ± 0.86	$3.91 \pm 1.12^{\#}\downarrow$	$3.22 \pm 1.32^{\#}\downarrow$	$5.42 \pm 1.52^{\#}$	$4.64 \pm 1.20^{\#}$
Degree of anisotropy (1)*	1.23 ± 0.14	1.69 ± 0.29	1.32 ± 0.25	1.50 ± 0.40	$2.03 \pm 0.29\uparrow$	$2.25 \pm 0.36\uparrow$	1.87 ± 0.80	1.98 ± 0.55
Structure model index (0–3)*	1.52 ± 0.27	1.42 ± 0.35	1.96 ± 0.20	1.80 ± 0.40	$2.08 \pm 0.27\uparrow$	$2.41 \pm 0.37\uparrow$	1.40 ± 0.43	1.52 ± 0.21
Trabecular number (1/mm)	1.17 ± 0.22	1.08 ± 0.16	0.92 ± 0.10	0.95 ± 0.07	0.91 ± 0.18	0.82 ± 0.27	1.05 ± 0.34	1.06 ± 0.16
Trabecular thickness (mm)	0.19 ± 0.04	0.17 ± 0.03	0.20 ± 0.01	0.22 ± 0.04	0.22 ± 0.04	0.20 ± 0.02	0.22 ± 0.05	0.24 ± 0.02
Trabecular spacing (mm)*	0.86 ± 0.12	0.76 ± 0.27	1.18 ± 0.13	1.11 ± 0.08	$1.20 \pm 0.28\uparrow$	$1.41 \pm 0.44\uparrow$	1.09 ± 0.34	0.95 ± 0.13

Note: "*" indicated significant difference between time zero and specific time point time postoperatively and "#" indicated significant difference between the femoral and tibial sides at the 0.05 level by two-way ANOVA; "↑" and "↓" indicated increase and decrease postoperatively in comparison with time zero by at the 0.05 level *post hoc* test.
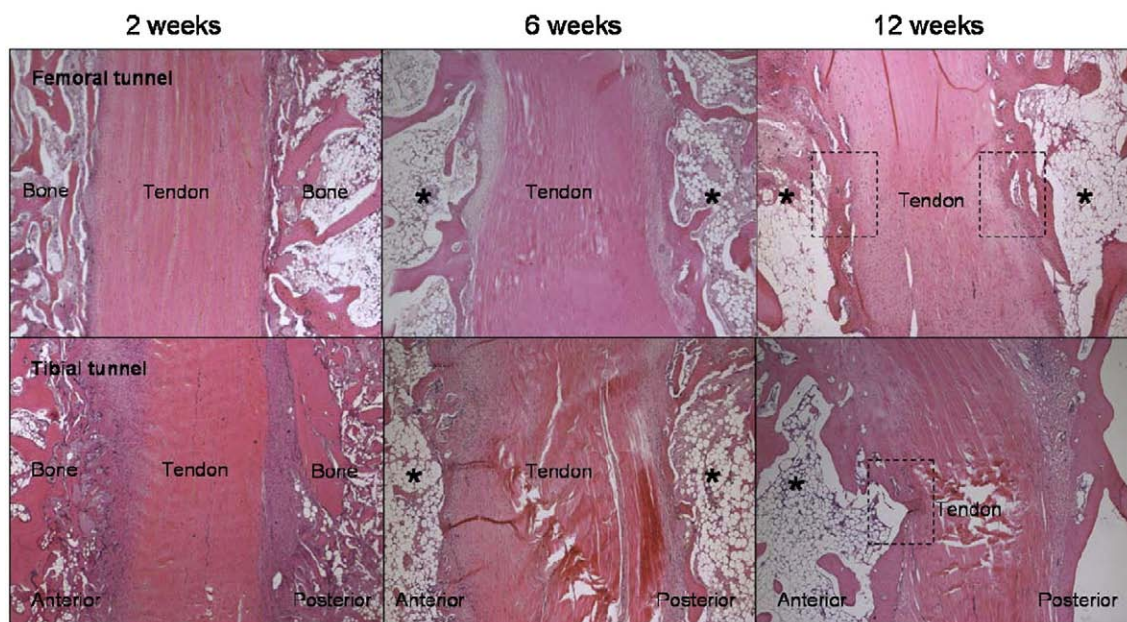
Fig. 4. The representative images showing the deterioration of peri-tendon bone (in dotted box) architecture on the tibial side within 6 weeks postoperatively. Newly-formed bone sheath was highly-oriented along the long axis of bone tunnel (arrow) and loosely connected with the residue bone (star).
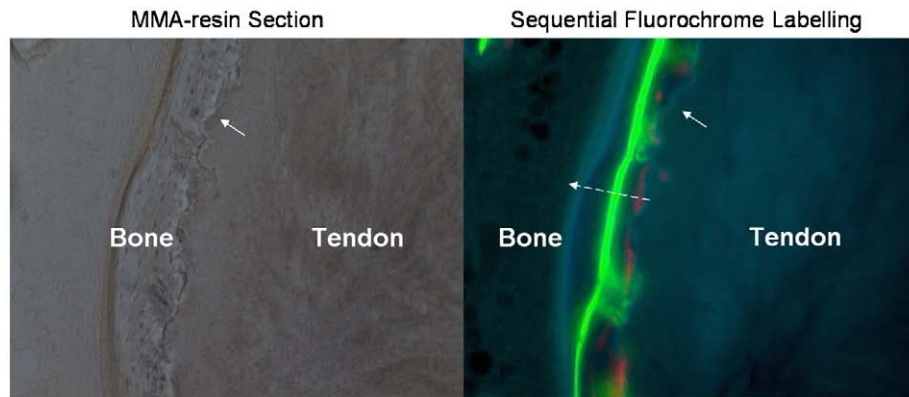
Aldrich GmbH) and calcium blue (30 mg/kg, from Grunthal GmbH) was injected subcutaneously and sequentially into the rabbits of 6-week group at week 3, 4, 5 and of 12-week group at week 9, 10, and 11, postoperatively. After euthanasia, the samples were dehydrated sequentially in ethanol and xylene and infiltrated with methylmethacrylate (MMA). The embedded specimens were sectioned perpendicularly to the bone tunnels by saw microtome (SP 1600, Leica, Germany). The sections in the middle portion of bone tunnel were grounded and polished to 80–100 μm by grinder/polisher (RotoPol-21, Struers, Denmark) for subsequent fluorescence microscopic examination.

Biomechanical testing

The femur–graft–tibia complexes were harvested and stored at − 20 °C until biomechanical testing within 1month after surgery. After the samples were thawed overnight at room temperature, the knee joints were carefully dissected to remove surrounding soft tissue until only ACL graft was left as the physical connection between femur and tibia. The fixation by suture on both sides was removed when testing. The graft–tunnel complexes were fixed with custom-made clamps, allowing tensile loading along the long axis of the graft

Fig. 5. The representative photographs showing temporal changes of peri-tendon bone and tendon-to-bone healing interface. Loss of surrounding trabeculae (star) was accompanied by new bone formation in the vicinity of the grafted tendon (dotted box) postoperatively. (Original magnification: 50×).

Fig. 6. The representative microphotographs showing the dynamic process of new bone formation in the vicinity of the grafted tendon on the tibial side. The red, green and blue line indicated new bone formation at 3, 4 and 5 weeks postoperatively of 6-week group. Bone grew into tendon substance (arrow); it also proceeded from tendon surface to the residual bone (arrows with dot line) (original magnification: 200×).

in a material testing machine (H25K-S, Hounsfield Test Equipment LTD, Surrey, UK).

A preload of 1N and a load displacement rate of 50mm/min tensile force were applied to the graft–tunnel complex until failure. The failure mode was recorded and the load to failure (N) and stiffness (N/mm) were calculated based on the load displacement curve.

Statistical analysis

The comparisons for BMD, tunnel area, peri-graft bone mass and microarchitecture among the different time points at distal femur and proximal tibia were performed using two-way ANOVA. When it indicated overall significance of main effects and without interaction between them, the difference between individual time points and sites was assessed by *post hoc* tests. The failure modes between the time points were also compared using Fisher's Exact test. Correlation of peri-graft bone mass and microarchitecture with mechanical properties of T–B attachment was done using Pearson's correlation. The level of significance was set at $p < 0.05$. All data analyses were performed using SPSS 15.0 analysis software (SPSS Inc., Chicago, IL, USA).

Results

pQCT evaluation

As showed in Fig. 3, transient bone mineral loss was observed on both the femoral and tibial sides after surgery. In comparison with time zero postoperatively, BMD at week 2 was slightly higher but not statistically significant. BMD at week 6 was significantly lower than that at time zero by 13.7% and 21.7% on the femoral and tibial sides respectively ($p < 0.05$ for both). Although BMD partially reversed at week 12, it was still significantly lower than that at time zero by 7.1% and 8.9% on the femoral and tibial sides respectively ($p < 0.05$ for both).

There was no significant difference in BMD between the femoral and tibial side at time zero. But BMD on the femoral side was higher than that on the tibial side at 6 weeks postoperatively. The femoral tunnel significantly enlarged at 6 weeks in comparison with that at time zero after surgery ($p = 0.037$) but there was no such difference shown in the area of the tibial tunnel (Fig. 3).
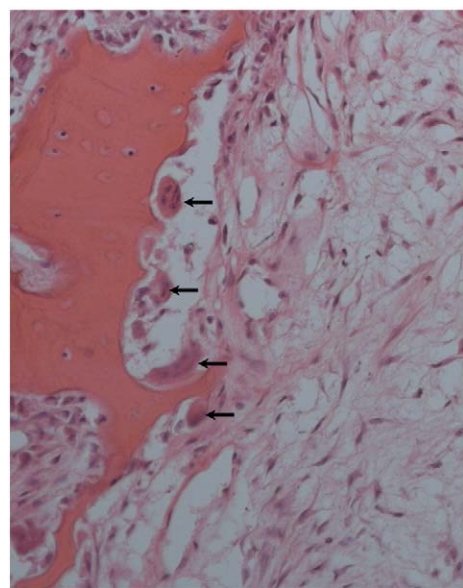
Micro-CT evaluation

As showed in Table 1, there were transient peri-graft bone mass decrease and microarchitecture deterioration postoperatively. The similar trend of changes was noted on the femoral and tibial sides. As showed in Fig. 4, peri-graft bone on the tibial side was loosely connected and composed of more rod-like trabeculae than plate-like trabeculae at 6 weeks after surgery, which was indicated by lower Con. D and higher SMI. The newly-formed bone in the vicinity of the grafted tendon was highly-oriented and anisotropic along the long axis of bone tunnel, which was indicated by higher DA.

There was no significant difference between the femoral and tibial sides in the fraction of BV/TV and bone connectivity in the vicinity of the grafted tendon at time zero. It was observed that peri-graft bone connectivity and BV/TV was inferior on the tibial side to those on the femoral side at 6 weeks postoperatively ($p < 0.05$ for both). Peri-graft bone connectivity on the tibial side was still lower than that on the femoral side at 12 weeks postoperatively ($p < 0.05$).
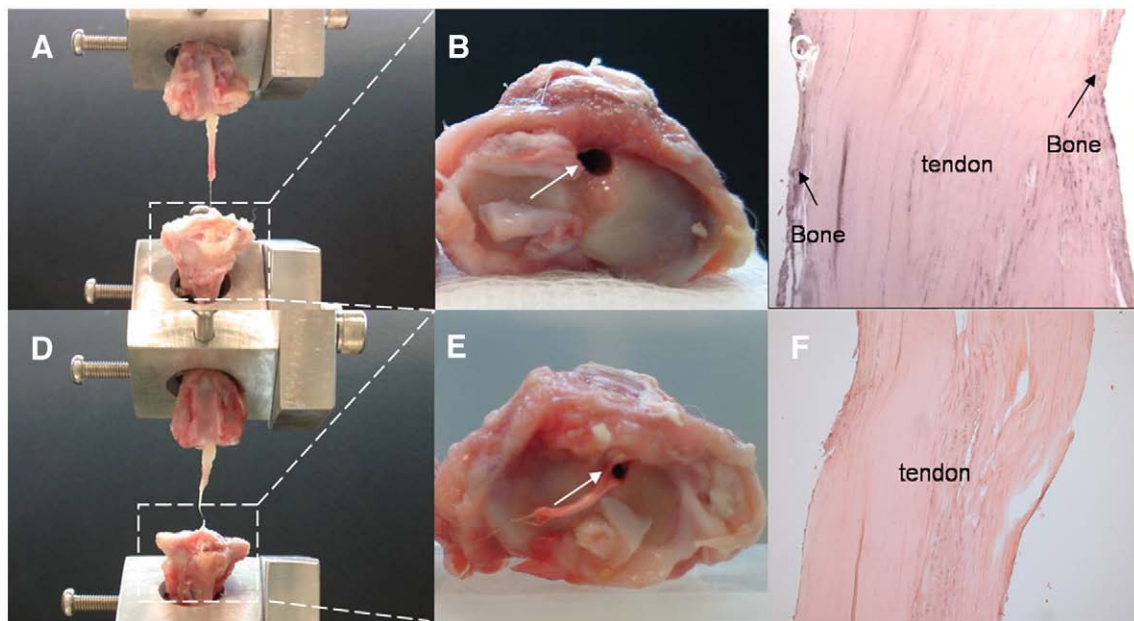
Decalcified and undecalcified histological examination

The boundary of T–B healing interface became obscure with peri-graft new bone formation with healing over time (Fig. 5). Under fluorescence microscopic examination, newly-formed bone grew into T–B healing interface and tendinous substance; it also gradually

Fig. 7. The representative microphotographs showing osteoclasts (arrows) accumulation on the surface of peri-graft bone in the tibial tunnel at 6 weeks after surgery (original magnification: 200×).

Fig. 8. The representative photographs showing failure mode of graft–tunnel complexes at 6 weeks (A–C) and 12 weeks (D–F) after surgery. (B and E) Grafted tendon was prone to be pulled out of the tibial tunnel. (C and F) The corresponding histological sections revealed that tendon graft was pulled out of bone tunnel with bone attachment (arrow) at 6 weeks postoperatively; it ruptured at intra-osseous tendon substance at 12 weeks after surgery (original magnification: 50×).

proceeded from the surface of grafted tendon to the host bone (Fig. 6). Higher mineral apposition rate was observed (17 ± 5 μm/week) in comparison with that at 12 weeks after surgery (11 ± 7 μm/week) ($p = 0.017$). Osteoclasts accumulated on the surface of peri-graft bone at 6 weeks after surgery and the pre-existing trabeculae decreased gradually (Fig. 7).

Biomechanical testing

Only one graft of the femur–graft–tibia complex at week 6 was pulled out from the femoral tunnel and the majority (7/8) was broken in the tibial tunnel. Microscopic examination revealed that the grafted tendon was pulled out from the tunnel together with a bony attachment (Fig. 8). The ultimate strength and stiffness of the complexes were 43 ± 11N and 15 ± 4N/mm respectively, which correlated with the statues of peri-graft bone mass and connectivity etc. (Table 2).

All eight samples ruptured in tendinous substance inside the tibial tunnel at week 12 postoperatively, which showed a different failure mode from that at week 6 ($p < 0.001$) (Fig. 8). The ultimate strength and stiffness of the complexes were 39 ± 14N and 16 ± 8N/mm respectively. The stiffness of the complexes correlated with peri-graft bone connectivity with statistical significance (Table 2).

Discussion

The present experimental study was designed to prove our hypothesis that the pull-out strength of T–B attachment was related to peri-graft bone mass and microarchitecture after ACL reconstruction. To our best knowledge, this study was the first one to systemically quantify the changes of bone mass and microarchitecture using the non-destructive advanced bioimaging tools, i.e. high-resolution multi-layer pQCT and micro-CT, to provide an insight into the biological behavior of tunneled bone and its relations to T–B attachment strength during healing.

Results from pQCT, micro-CT and histological examination showed transient peri-graft bone loss with its microarchitecture deterioration after ACL reconstruction. It was noted that the decrease of peri-graft BMD, BV/TV and bone connectivity were more severe on the tibial side, and its peri-graft bone quality and quantity was inferior to that on the femoral side at week 6 after surgery, although there was no significant difference between them at time zero. The healing quality of T–B attachment was influenced by peri-graft bone mass [3]. It may result in that the grafted tendon was prone to be pulled out of the tibial tunnel with a lower bone mass at week 6. In addition, such bone loss was accompanied by new bone formation in the vicinity of the grafted tendon. Histological examinations revealed that peri-graft

Table 2
Correlations between mechanical properties of graft–tunnel complexes and peri-tendon bone mass and microarchitecture.

Pearson correlation			Bone volume/ tissue volume	Degree of anisotropy	Connectivity density	Structure model index	Trabecular number	Trabecular thickness	Trabecular spacing
6 weeks	Ultimate strength (N)	r^2	0.524[a]	−0.227	0.283[b]	−0.120	0.004	0.338[a]	−0.066
		p value	0.008	0.118	0.075	0.270	0.848	0.047	0.421
	Stiffness (N/mm)	r^2	0.682[a]	−0.404[a]	0.473[a]	−0.338[a]	0.025	0.484[a]	−0.010
		p value	0.001	0.026	0.013	0.048	0.627	0.012	0.321
12 weeks	Ultimate strength (N)	r^2	0.634[b]	−0.006	0.203	−0.174	0.018	0.608[b]	−0.097
		p value	0.058	0.884	0.136	0.41	0.799	0.067	0.547
	Stiffness (N/mm)	r^2	0.616[b]	−0.006	0.407[a]	−0.371[a]	0.084	0.709[a]	−0.257
		p value	0.064	0.761	0.037	0.012	0.577	0.036	0.305

[a] Correlation was significant at the 0.05 level (2-tailed).
[b] Correlation was insignificant but showed a trend at the 0.1 level (2-tailed).

bone connectivity between newly-formed bone and pre-existing bone was not well established with healing over time. This may explain the observations on the pull-out of grafted tendon with bone attachment and significant association of the stiffness of T–B attachment with the peri-graft bone connectivity at both week 6 and 12 after surgery. Thus, it would be helpful to monitor the changes of peri-graft bone mass and microarchitecture for prediction of T–B healing.

It was known that T–B healing interface was the weakest point of a graft–tunnel complex immediately after ACL reconstruction [18]. In this experimental study, we systemically described the temporal changes of this weakest point with healing over time. Peri-graft bone loss may result in a paradigm shift from T–B interface at time zero to peri-graft bone at 6 weeks after surgery. With partial reverse of peri-graft bone, the weakest point of the complexes shifted to intra-osseous tendon substance. It was considered that maintaining or fortifying peri-tendon bone was of importance for providing stable T–B anchorage sites. Understanding of the factors influencing dynamic changes of peri-tendon bone would be helpful for making a therapeutic strategy to enhance T–B healing and improve the outcome of ACL reconstruction.

Changes of peri-tendon bone were influenced by both mechanical and biological factors in local milieus. A finite element analysis showed that tunnel creation led to stress shielding of host bone, which resulted in bone resorption [19]. Histologically, we observed accumulation of osteoclasts at the surface of peri-graft bone, explaining the loss of peri-graft trabeculae in the early T–B healing phase. This was also supported by similar findings reported previously [5,20]. Moreover, a clinical study found that under magnetic resonance imaging (MRI) examination synovial fluid influx was prone to occur in the tibial tunnel [21], which might interfere with tunneled bone healing and aggravate bone loss on the tibial side [22]. It may result in the disparity of healing on the femoral and tibial sides that peri-graft bone mass and connectivity on the tibial side was inferior to those on the femoral side at 6 and 12 weeks postoperatively, yet without significant difference at time zero. These findings were of great clinical significance as they suggested that T–B healing, particularly in the tibial tunnel should be especially targeted for healing enhancement.

Tendon/ligament repair in bone tunnel was considered to be advantageous for a large contact surface and exposure to mesench-ymal stem cells (MSCs) in bone marrow in comparison with a direct T–B appositional repair [2]. Actually, shearing force existed across T–B healing interface, which was different from a physiological tensile force across a native tendon/ligament-to-bone attachment [23]. Temporal changes of peri-graft bone microarchitecture reflected the deleterious effect of such non-physiological condition. The present study showed that surrounding trabeculae became anisotropic and highly-oriented along the long axis of tendon. Moreover, those consisted of more rod-like trabeculae than plate-like ones, which indicated less maturation of peri-graft bone microarchitecture. The strength of a native ACL-to-bone attachment of rabbit was around 400N (*unpublished data*) and T–B attachment strength only reached 1/10 of a native L–B attachment at 12 weeks after surgery. As showed in our previous studies, T–B appositional repair strength reached over 1/5 of that of a native one at 12 weeks postoperatively in a partial patellectomy rabbit model [24–27]. Similar comparison was also performed by Silva et al. who demonstrated that tunnel repair was mechanically and histologically inferior to direct appositional repair in a phanlangeal bone of canine [4]. Recently, it was reported that grafted tendon was pre-conditioned towards to osteogenesis before implantation into bone tunnel using bone morphogenetic protein-2 (BMP-2) and to turn T–B healing into bone-to-bone healing, which improved the T—B attachment strength in an extra-articular tibial tunnel in rabbit [28].

The present study showed that the femoral tunnel area tended to be larger with healing over time while the tibial tunnel area did not change over time. However, histological findings showed that newly-formed bone grew into T–B healing interface and tendinous substance in both the femoral and tibial tunnel. These findings suggested that there was no direct relationship between bone tunnel area or diameter and healing at T–B interface. This might explain why tunnel enlargement was not in relation to knee function after surgery shown in the majority of clinical studies in the past decade [29]. This implied that the parameter of tunnel diameter on plain X-ray were not reliable to predict T–B healing and its attachment strength.

In summary, T–B attachment strength was associated with peri-graft bone mass and connectivity. Our findings suggested that pQCT and micro-CT might provide a more accurate and comprehensive information on changes of host bone and provide better prediction of T–B healing in bone tunnel than the conventional plane radiographic method.

Acknowledgments

References

[1] Woo SL, Wu C, Dede O, Vercillo F, Noorani S. Biomechanics and anterior cruciate ligament reconstruction. J Orthop Surg 2006;1:2.
[2] Deehan DJ, Cawston TE. The biology of integration of the anterior cruciate ligament. J Bone Joint Surg Br 2005;87:889–95.
[3] Grassman SR, McDonald DB, Thornton GM, Shrive NG, Frank CB. Early healing processes of free tendon grafts within bone tunnels is bone-specific: a morphological study in a rabbit model. Knee 2002;9:21–6.
[4] Silva MJ, Thomopoulos S, Kusano N, Zaegel MA, Harwood FL, Matsuzaki H, et al. Early healing of flexor tendon insertion site injuries: tunnel repair is mechanically and histologically inferior to surface repair in a canine model. J Orthop Res 2006;24:990–1000.
[5] Ditsios K, Boyer MI, Kusano N, Gelberman RH, Silva MJ. Bone loss following tendon laceration, repair and passive mobilization. J Orthop Res 2003;21:990–6.
[6] Moffat KL, Sun WS, Chahine NO, Pena PE, Doty SB, Hung CT, et al. Characterization of the mechanical properties and mineral distribution of the anterior cruciate ligament-to-bone insertion site. Conf Proc IEEE Eng Med Biol Soc 2006; 1:2366–9.
[7] Milz S, Rufai A, Buettner A, Putz R, Ralphs JR, Benjamin M. Three-dimensional reconstructions of the Achilles tendon insertion in man. J Anat 2002;200: 145–52.
[8] Benjamin M, Toumi H, Suzuki D, Redman S, Emery P, McGonagle D. Microdamage and altered vascularity at the enthesis-bone interface provides an anatomic explanation for bone involvement in the HLA-B27-associated spondylarthritides and allied disorders. Arthritis Rheum 2007;56:224–33.
[9] Doschak MR, Wohl GR, Hanley DA, Bray RC, Zernicke RF. Antiresorptive therapy conserves some periarticular bone and ligament mechanical properties after anterior cruciate ligament disruption in the rabbit knee. J Orthop Res 2004;22: 942–8.
[10] Doschak MR, LaMothe JM, Cooper DM, Hallgrimsson B, Hanley DA, Bray RC, et al. Bisphosphonates reduce bone mineral loss at ligament entheses after joint injury. Osteoarthr Cartil 2005;13:790–7.
[11] Benjamin M, Kumai T, Milz S, Boszczyk BM, Boszczyk AA, Ralphs JR. The skeletal attachment of tendons—tendon "entheses". Comp Biochem Physiol A Mol Integr Physiol 2002;133:931–45.
[12] Wen, CY, Qin, L, Lee, SK, Chan, KM, The use of brushite calcium phosphate cement for enhancement of bone-tendon integration-in an anterior cruciate ligament reconstruction rabbit model. J Biomed Mater Res B Appl Biomater (2008), doi:10.1002/jbm.b.31236.
[13] Wang CJ, Wang FS, Yang KD, Weng LH, Sun YC, Yang YJ. The effect of shock wave treatment at the tendon–bone interface—an histomorphological and biomechanical study in rabbits. J Orthop Res 2005;23:274–80.
[14] Thomopoulos S, Matsuzaki H, Zaegel M, Gelberman RH, Silva MJ. Alendronate prevents bone loss and improves tendon-to-bone repair strength in a canine model. J Orthop Res 2007;25:473–9.
[15] Siu WS, Qin L, Cheung WH, Leung KS. A study of trabecular bones in ovariectomized goats with micro-computed tomography and peripheral quantitative computed tomography. Bone 2004;35:21–6.
[16] Yingjie H, Ge Z, Yisheng W, Ling Q, Hung WY, Kwoksui L, et al. Changes of microstructure and mineralized tissue in the middle and late phase of osteoporotic fracture healing in rats. Bone 2007;41:631–8.

[17] Lu H, Qin L, Fok P, Cheung W, Lee K, Guo X, et al. Low-intensity pulsed ultrasound accelerates bone–tendon junction healing: a partial patellectomy model in rabbits. Am J Sports Med 2006;34:1287–96.
[18] Magen HE, Howell SM, Hull ML. Structural properties of six tibial fixation methods for anterior cruciate ligament soft tissue grafts. Am J Sports Med 1999;27:35–43.
[19] Au AG, Raso VJ, Liggins AB, Otto DD, Amirfazli A. A three-dimensional finite element stress analysis for tunnel placement and buttons in anterior cruciate ligament reconstructions. J Biomech 2005;38:827–32.
[20] Kawamura S, Ying L, Kim HJ, Dynybil C, Rodeo SA. Macrophages accumulate in the early phase of tendon–bone healing. J Orthop Res 2005;23:1425–32.
[21] Clatworthy MG, Annear P, Bulow JU, Bartlett RJ. Tunnel widening in anterior cruciate ligament reconstruction: a prospective evaluation of hamstring and patella tendon grafts. Knee Surg Sports Traumatol Arthrosc 1999;7:138–45.
[22] Berg EE, Pollard ME, Kang Q. Interarticular bone tunnel healing. Arthroscopy 2001;17:189–95.
[23] Yamakado K, Kitaoka K, Yamada H, Hashiba K, Nakamura R, Tomita K. The influence of mechanical stress on graft healing in a bone tunnel. Arthroscopy 2002;18:82–90.

[24] Lu H, Qin L, Lee K, Wong W, Chan K, Leung K. Healing compared between bone to tendon and cartilage to tendon in a partial inferior patellectomy model in rabbits. Clin J Sport Med 2008;18:62–9.
[25] Wang L, Qin L, Lu HB, Cheung WH, Yang H, Wong WN, et al. Extracorporeal shock wave therapy in treatment of delayed bone–tendon healing. Am J Sports Med 2008;36:340–7.
[26] Wang W, Chen HH, Yang XH, Xu G, Chan KM, Qin L. Postoperative programmed muscle tension augmented osteotendinous junction repair. Int J Sports Med 2007;28:691–6.
[27] Leung KS, Qin L, Fu LK, Chan CW. A comparative study of bone to bone repair and bone to tendon healing in patella–patellar tendon complex in rabbits. Clin Biomech (Bristol, Avon) 2002;17:594–602.
[28] Hashimoto Y, Yoshida G, Toyoda H, Takaoka K. Generation of tendon-to-bone interface "enthesis" with use of recombinant BMP-2 in a rabbit model. J Orthop Res 2007.
[29] Wilson TC, Kantaras A, Atay A, Johnson DL. Tunnel enlargement after anterior cruciate ligament surgery. Am J Sports Med 2004;32:543–9.